IRSTI 29.19.22 https://doi.org/10.26577/ijmph.20261712

PREPARATION OF TRANSPARENT SUPERHYDROPHOBIC COATINGS WITH ANTI-ICING, ANTI-FOGGING AND SELF-CLEANING PROPERTIES BY PLASMA POLYMERISATION AT ATMOSPHERIC PRESSURE

B.A. Kyrykbay [1,3], **S.S. Ussenkhan** [1,3], **N.Ye. Akhanova** [1], **A.U. Utegenov** [2,3*], **M.T. Gabdullin** [1,2] **and S.A. Orazbayev** [2,3]

[1] *Kazakh-British Technical University, Almaty, Kazakhstan*
[2] *Al-Farabi Kazakh National University, Almaty, Kazakhstan*
[3] *Institute of Applied Sciences and Information Technologies, Almaty, Kazakhstan*

Email: almasbek@physics.kz

(Received 17 December 2025; revised 12 March 2026; accepted 12 May 2026)

Abstract. This study analyses the stability of superhydrophobic coatings produced by plasma polymerisation at atmospheric pressure using argon (Ar) as the base gas and hexamethyldisiloxane (HMDSO) as the precursor. The evaluation was aimed at determining the strength and durability of these coatings when exposed to various environmental factors such as fogging, anti-icing and temperature fluctuations. The superhydrophobic properties of the coatings were investigated by measuring contact angles and surface roughness values. The results show that the coatings obtained by the above mentioned method have significant water repellent property and retain their superhydrophobic characteristics for a long time. The results indicate that the combination of Ar and HMDSO in plasma polymerisation at atmospheric pressure is a promising approach to create stable and durable superhydrophobic surfaces suitable for various applications. The main focus is on the stability of coatings, their ability to resist icing and fogging. The study showed that the hydrophobic properties of the coatings can be improved by optimising the process parameters, resulting in coatings with a water contact angle of more than 154 ± 2 degrees and high transparency of up to 98.5% in the visible range. The obtained results testify to the high efficiency of the proposed method of obtaining coatings, which opens up prospects for their application in various fields where high resistance and transparency to external influences are required.

Keywords: plasma polymerization, atmospheric pressure, superhydrophobic coatings.

INTRODUCTION

Superhydrophobic surfaces, known for their exceptional water repellent properties [1], have the ability to repel water so that it accumulates and rolls off, resembling mercury droplets. Such coatings are valued for their multifunctional properties including water resistance [2], self-cleaning [3], corrosion protection [4], anti-fogging [5], anti-icing [6] and biofouling prevention [7–9]. In recent years, superhydrophobic surfaces (contact angle (CA) greater than 150°, sliding angle (SA) less than 10°) created by nature have attracted considerable interest from researchers due to their exceptional hydrophobic properties [10]. Such surfaces are known to possess two key characteristics: micro/nanoscale roughness and low surface energy. They show high potential for applications in various fields such as self-cleaning [11], concrete protection [12], oil/water separation [13–15], anti-icing [16], anti-corrosion coatings [17–19], and biomedicine.

Usually, superhydrophobic surfaces are created in two main ways: by forming a rough structure using low surface energy materials or by pre-treating the rough structure and then modifying it with low surface energy materials. Many methods have been developed to obtain a surface with a high degree of roughness, including sol-gel method [20], chemical vapour deposition [21,22] and electrodeposition [23]. However, large-scale production of such surfaces still faces difficulties due to complex processes and high equipment costs. A key challenge in this area is the efficient and cost-effective production of such coatings on a large scale. Conventional methods such as chemical vapour deposition [24–26]

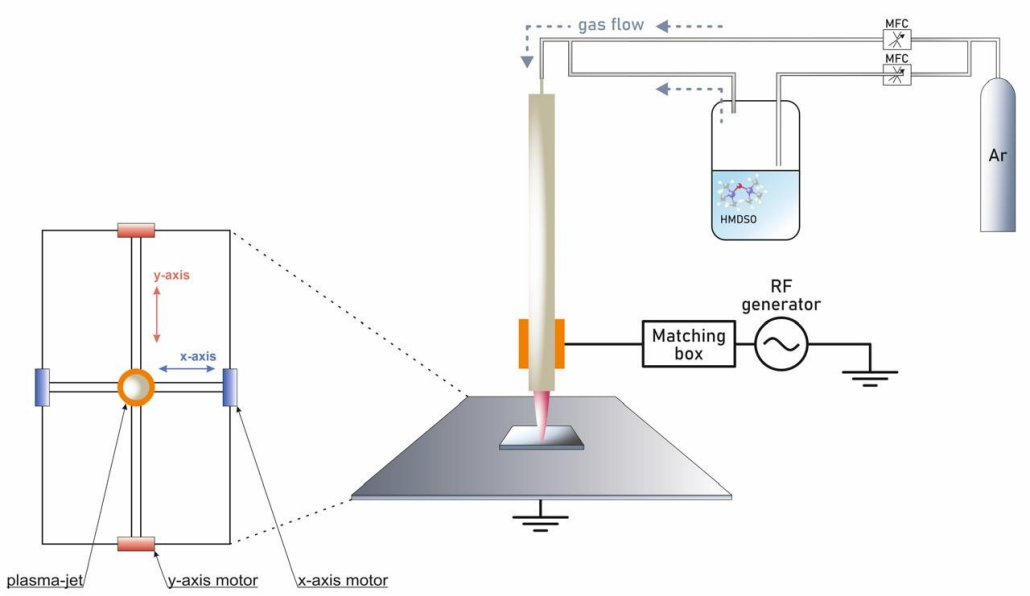

Figure 1 - Scheme of experimental setup.

and plasma polymerisation [27–30], while effective, often involve complex processes, expensive equipment and potentially harmful chemicals.

In this regard, plasma polymerisation at atmospheric pressure using argon and HMDSO is becoming a promising alternative [31]. This method simplifies the deposition process, eliminating the need for high vacuum and reducing the need for hazardous chemicals, offering an environmentally friendly and cost-effective solution.

In addition, the integration of 3D plotter technology, such as the CNC3018, increases the practicality of applying superhydrophobic coatings to large areas [32]. This technology enables coatings to be applied to a variety of materials in a cost-effective manner, providing a scalable and efficient approach for industrial applications. The use of a 3D plotter can produce homogeneous and durable coatings without the significant costs associated with traditional methods.

This study investigates the stability of superhydrophobic coatings created using Ar and HMDSO at atmospheric pressure, with a focus on anti-icing and anti-fogging. The results highlight the advantages of combining atmospheric pressure plasma polymerisation and 3D plotter technology, offering large-scale and cost-effective production of superhydrophobic surfaces.

Experimental Section

Fig. 1 shows a schematic of the setup used to study the coating formed by a plasma jet generated by a radio-frequency discharge at atmospheric pressure. The plasma jet was generated by means of a radio-frequency generator, which was placed between a copper wire enclosed in a quartz tube and a grounded copper plate. The quartz tube was 100 mm long, with an inner diameter of 3 mm and an outer diameter of 10 mm. A 13.56 MHz Seren-R 301 radio frequency generator model was used as the power source. The main gas stream consisted of argon (Ar) and the precursor HMDSO. Since HMDSO is liquid at room temperature, a small amount was added to the bubbled. The gas supply was regulated by means of a mass flow controller. The CNC3018 plotter has a maximum speed of 80 mm/s. The coating samples were deposited on 2×2 cm glass substrates, which were pre-cleaned in an ultrasonic bath for 10 min. At the beginning of the experiment, a gas mixture of Ar and HMDSO was fed into the quartz tube, after which an atmospheric pressure plasma was initiated by applying a high-frequency voltage to the outer electrode. In the plasma phase, chemical reactions and coagulation of atoms took place leading to the formation of the nanocoating. The experiment

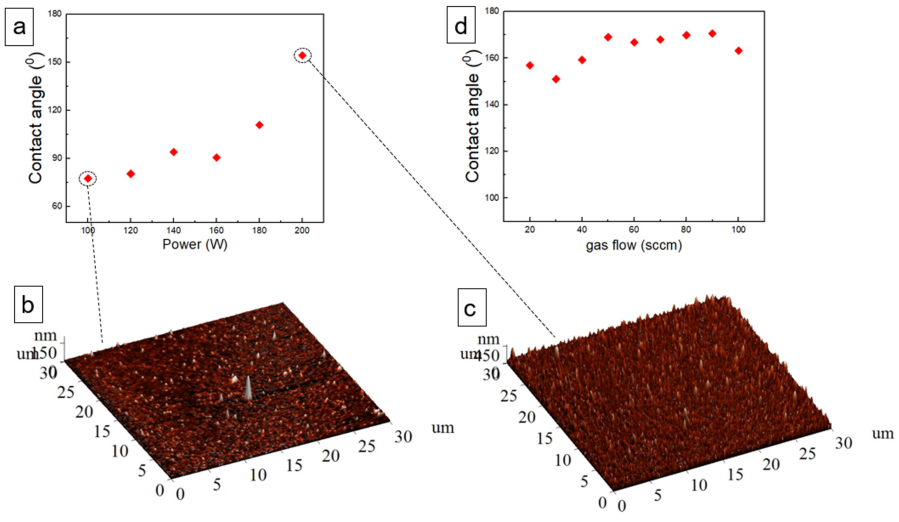

Figure 2 - Graphs of contact angle versus discharge power (a) and gas flow (d). AFM images of the sample, at 100 W power (b) and at 200 W power (c).

was carried out at a plasma power of 200 W and a HMDSO/Ar ratio, where 98% was Ar and 2% HMDSO.

Characterisation Methods

All samples were examined in a controlled laboratory environment. The surface morphology of the obtained specimens was investigated using a scanning electron microscope (Quanta 3D 200i, SEM FEIcompany) and an atomic force microscope (NTEGRA THERMA NT-MDT AFM). The optical characteristics of the thin films were assessed with a UV-Vis spectrophotometer (Cary 5000 UV-Vis-NIR Spectrophotometer). The contact angle measurements were performed with a Contact Angle Goniometer (Ossila).

Results and Discussion

In the course of the study, experiments aimed at finding optimal conditions for the formation of transparent superhydrophobic coatings were carried out. In the first stage of the work, the dependence of the contact angle of the films on the discharge power was studied. The gas flows of argon (Ar) and argon-HMDSO mixture were kept constant and were 40 sccm and 20 sccm, respectively. The maximum speed of the plotter was 80 mm/s. The discharge power (Fig. 2a) was varied from 100 to 200 W in steps of 20 W, after which the water contact angles on the surface of the formed coatings were measured. With an increase in discharge power, a significant change in the surface morphology of the samples is observed. Fig. 2b shows an AFM image of the surface treated at 100 W power, which demonstrates a relatively smooth structure with minor variations in topography. The surface roughness was evaluated in terms of the average roughness (R_a) and the root mean square roughness (R_q, RMS). Based on the topographical contrast, the roughness values are estimated to be in the range of $R_a \approx 8.3 \pm 0.2$ nm and $R_q \approx 10.8 \pm 1.5$ nm, indicating a relatively uniform surface morphology. However, when the power is increased up to 200 W (Fig. 2c), nanostructures grow, resulting in an increase in surface micro-roughness. This is due to the fact that an increase in the discharge power enhances the energy of ions and active species in the plasma, thereby intensifying deposition processes and promoting the formation of more pronounced nanostructures on the surface. As a consequence, the surface roughness increases, with $R_a \approx 15 \pm 1.4$ nm and $R_q \approx 20.3 \pm 6.5$ nm, indicating a significant enhancement of surface texturing compared to the 100 W condition. At low power levels, the deposited layer has a homogeneous and smooth surface, whereas at high discharge power levels,

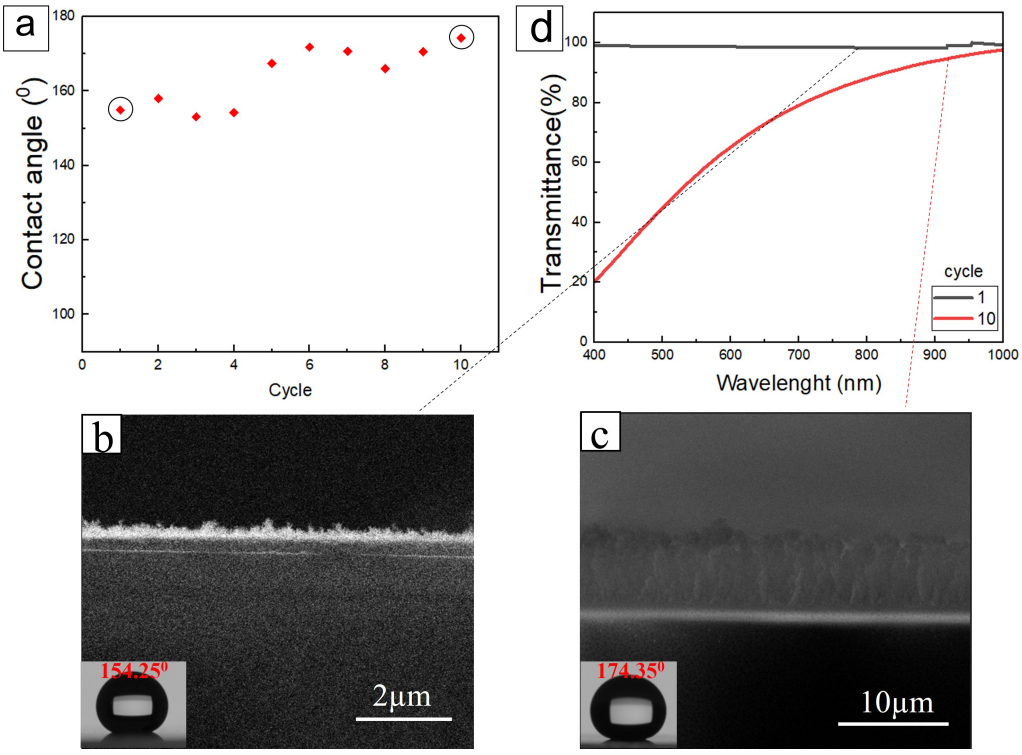

Figure 3 - Graphs of contact angle versus gas flow rate (a). SEM images of the surface of films deposited on a silicon substrate by plasma polymerisation at atmospheric pressure after one (b) and ten (c) cycles. Graphs of transmission coefficient dependence on the number of cycles (d).

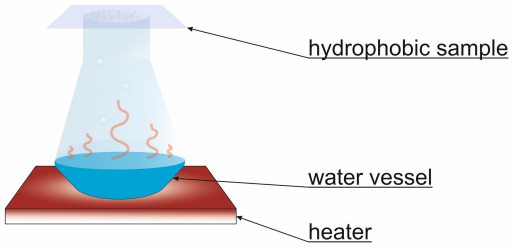

Figure 4 - Modelling scheme of the fogging protection test.

pronounced nanostructures are formed, contributing to an increase in the micro-roughness of the coating. Analysis of the graphs (Fig. 2d) shows that the wetting angle is maintained in the range from 150° to 180° when the Ar+HMDSO mixture flux is changed. These results indicate that changing the Ar+HMDSO flux does not significantly affect the hydrophobic properties of the formed coatings. Therefore, the following experiments will be performed at a set flux of 20 sccm Ar+HMDSO at a fixed discharge power of 200 W. The study of optical and superhydrophobic properties of the films was carried out at the maximum speed of the CNC3018 plotter - 80 mm/s. The following parameters were used during the experiments: discharge power - 200 W, pulsation frequency - 1000 Hz, argon main flow - 40 sccm, argon secondary flow - 20 sccm and HMDSO was maintained at room temperature. The effect of the number of deposition cycles on the wetting angle and transparency of the film was also investigated. In the experiment, the number of deposition cycles was varied from 1 to 10, (Fig. 3a) which revealed that the wetting angle increases from 154.25° to 174.35° with increasing number of cycles. According to the data presented in the SEM images of the surface, the morphology of the films obtained as a result of one and ten depo-

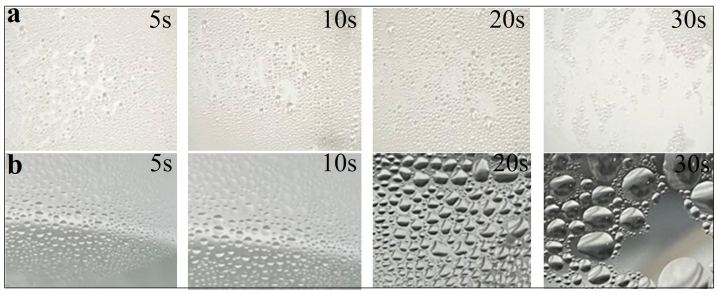

Figure 5 - Misting process of the test surfaces. Self-destruction of the collected drop using the Self-jump strategy (a). For comparison, a collected droplet on a conventional glass surface gradually transforms into larger droplets(b).

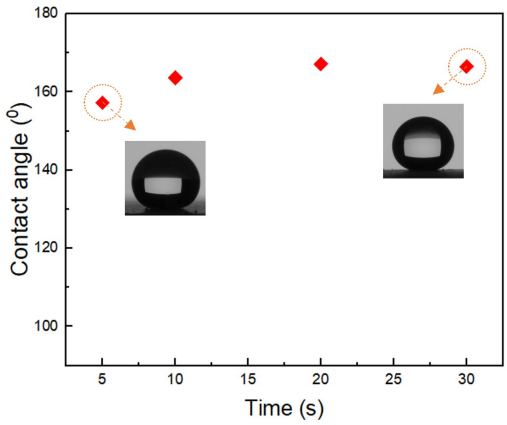

Figure 6 - Graph of dependence of misting time on contact angle.

sition cycles is practically unchanged. This situation confirms the stability of the superhydrophobic properties and wetting angle of the films at different numbers of cycles. However, the film thickness measurements show significant differences between the samples obtained after one and ten cycles. The thickness of the film obtained in one cycle is about 400 ± 50 nm (Fig. 3b), whereas it reaches about 6.3 μm (Fig. 3c) for the sample obtained after ten cycles. To investigate the effect of the number of deposition cycles on optical transparency, UVVis analysis was performed for samples obtained after 1 and 10 deposition cycles, relative to bare glass (Fig. 3d). The optical transparency of the coatings is closely related to the film thickness. As the number of deposition cycles increases, the thickness of the deposited layer also increases. As a result, the overall optical transparency decreases with increasing film thickness [17]. In contrast, the coating obtained after a single deposition cycle exhibits a transmittance of up to 98.5% in the visible region of the spectrum, which can be explained by its lower thickness. At the same time, it maintains superhydrophobic properties with a water contact angle of 154.25°, which corresponds to the preservation of the required surface roughness. These observations are directly confirmed by SEM and AFM results.

Investigation of the Stability of Hydrophobic Coatings

The experimental setup for the anti-fogging test is shown in Fig. 4 [37]. A round flask filled with water was used to evaluate the anti-fogging properties. The water was brought to boiling by heating the vessel to 200°C, after which the sample was placed in the neck of the round flask. The test was conducted for 30 seconds at cyclic intervals of 5 seconds each. The contact angle of the

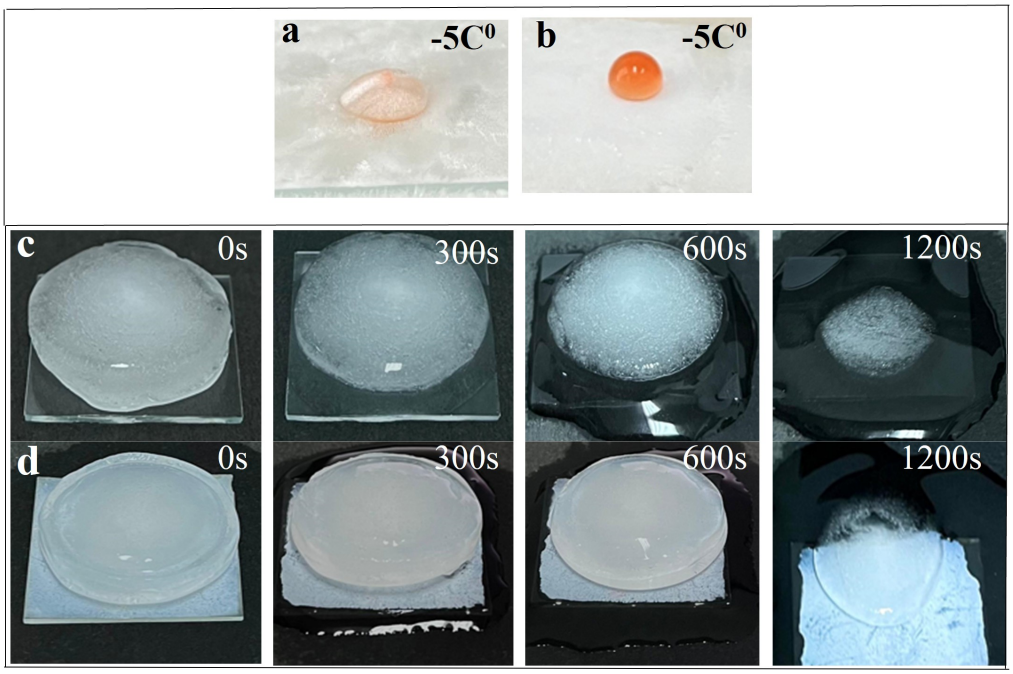

Figure 7 - Resistance of de-icing surfaces: to the freezing process on a conventional glass surface (a), on glass with superhydrophobic coating (b). Photographs of ice melting on different surfaces: plain glass (c), glass with superhydrophobic coating (d).

drop on the sample surface was measured, and its anti-fogging properties were evaluated by the degree of image clarity through the sample exposed to steam.

When fog droplets merge, the superhydrophobic surface causes them to bounce back (Fig. 5a). This property indicates that superhydrophobic surfaces are highly effective in fogging control. The droplet size on such surfaces is less than 0.3 mm, which favours self-cleaning due to the roughness of the surface, preventing the accumulation of large droplets and their formation [37]. The small water droplets collected on the surface gradually merge into large droplets. However, since small droplets cannot slide freely from the surface, they start to fall under gravity only after reaching a critical volume under gravity (Fig. 5b). This indicates an insufficient anti-fogging effect of the surface. However, such surfaces show high efficiency as thermal substrates because the water removal process favours efficient mass and energy transfer.

Fig. 6 shows a graph of the dependence of the contact angle on the fogging time. The experiment was conducted at intervals from 5 to 30 seconds. The graph shows a slight increase in the contact angle from 157.24° at 5 sec to 165° at 30 sec, which is within the error of the measuring device. This result indicates a high resistance of the surface to misting.

The study of the resistance of de-icing surfaces is presented in Fig. 7. Firstly, two samples were prepared: the first was ordinary clear glass and the second was glass coated with a superhydrophobic coating. A drop of water was applied to the surface of each sample and then cooled to −5°C. As a result, the water drop froze (Fig. 7a and 7b). After water freezing on the surface of the glass coated with the superhydrophobic layer, re-melting did not cause a change in the contact angle, indicating a high level of resistance of the coating to the de-icing process. The next stage of testing was the process of ice melting on both surfaces. For this purpose, ice was placed on the two glass surfaces and the process was observed (Fig. 7c). When exposed to heat, the ice melted

Table 1 – Comparative Performance of Plasma-Polymerised HMDSO-Based Hydrophobic Coatings Reported in the Literature

Method	Substrate	Precursor / Gas	Process	WCA	Optical Transmittance	Durability
This work	Glass	HMDSO+Ar	Atmospheric pressure RF plasma; controlled deposition cycles	156°	98%	icing cycles, fogging test
Atmospheric Plasma Spraying [33]	Al_2O_3–13%TiO_2	SPS-SiO2	SL-AP/SPS-SiO2 coating	158°	Not focused on optical properties	Abrasion resistance, Anti-icing
kHz plasma jet deposition (N_2 shielding influence) [34]	Glass	HMDSO + Ar	HMDSO	168°	90%	Not tested
HMDSO plasma polymerisation (low pressure) [35]	Glass / dielectric	HMDSO	Low-pressure plasma	158°	Not focused on optical properties	retained after 15 icing/de-icing cycles
Atmospheric plasma polymerization [36]	Metal / polymer	HMDSO	DBD plasma	90°	Not focused on optical properties	Not tested

and the water produced by the melting process collected on the glass surface. No water remained on the surface of the sample coated with the superhydrophobic coating, which contributed to the anti-icing properties of the coating. The superhydrophobic properties of the coating allowed water to roll off easily (Fig. 7d), resulting in self-cleaning of the surface and a reduction of residual ice on the sample. Table 1 summarises the performance of the developed atmospheric-pressure RF plasma coating in comparison with previously reported HMDSO-based plasma-polymerised coatings. The comparison includes key parameters such as substrate type, precursor system, processing conditions, water contact angle (WCA), optical transmittance, and durability characteristics.

The coating developed in this work demonstrates a high optical transmittance of 98% combined with a hydrophobic behaviour (WCA $\approx$ 156°), while being fabricated under atmospheric pressure using controlled deposition cycles. Compared to similar atmospheric plasma jet approaches (WCA $\approx$ 160°), the present method offers improved optical transparency and scalable deposition control. In contrast, low-pressure plasma systems show comparable wettability (WCA $\approx$ 158°) but require vacuum processing and focus primarily on icephobic durability rather than optical performance. Overall, the comparative analysis highlights the balanced multifunctional performance of the developed coating, which combines high transparency, hydrophobicity, and functional durability under atmospheric conditions.

Conclusions

The study comprehensively evaluated the stability of superhydrophobic coatings produced by plasma polymerisation at atmospheric pressure using argon (Ar) as the base gas and HMDSO as the precursor. The focus was on their resistance to environmental factors such as icing, fogging and temperature variations. Experiments confirmed the significant water repellency of the coatings

and their long-term retention of superhydrophobic properties. Optimisation of the process parameters allowed to achieve water repellent properties with wetting angle over 154 ± 2 degrees and transparency up to 98.5% in the visible range. The results indicate the high efficiency of this method of obtaining coatings, which opens up prospects for their application in various fields requiring high resistance to external influences and transparency. Further research could be directed towards optimising their application technologies and expanding their scope of use.

Acknowledgments

This research was funded by the Committee of Science of the Ministry of Science and Higher Education of the Republic of Kazakhstan (Grant No. BR27197639).

Author contributions: Kyrykbay B.A.: investigation, data curation, formal analysis, methodology, visualization, validation, writing original draft. Ussenkhan S.S.: investigation, methodology. N.Ye. Akhanova: resources, methodology. Utegenov A.U.: conceptualization, methodology, supervision, project administration, funding acquisition, writing review and editing. Gabdullin M.T.: resources, methodology, writing review and editing. Orazbayev S.A.: resources, methodology. All authors have read and agreed to the published version of the manuscript.

References

[1] Shahzadi, S., N. Nadeem, A. Javid, Y. Nawab, and Z. U. "Strategic insights into realizing superhydrophobic surfaces on cellulosic substrates through conventional and sustainable technologies." *Surfaces and Interfaces* 53 (2024): 105034. https://doi.org/10.1016/j.surfin.2024.105034

[2] Dong, X., B. Wan, D. Feng, Y.and Min, M.-S. Zheng, H. Xu, Z.-M. Dang, G. Chen, and J.-W. Zha. "Ultra-low-permittivity, high hydrophobic, and excellent thermally stable fluoroelastomer/polyimide composite films employing dielectric reduction." *European Polymer Journal* 181 (2022): 111667. https://doi.org/10.1016/j.eurpolymj.2022.111667

[3] Du, J., P. Wu, H. Kou, P. Gao, Y. Cao, J. L., S. Wang, P. Rusinov, and C. Zhang. "Self-healing superhydrophobic coating with durability based on ep + pdms/sio double-layer structure design." *Progress in Organic Coatings* 190 (2024): 108359. https://doi.org/10.1016/j.porgcoat.2024.108359

[4] Ma, C., L. Wang, A. Nikiforov, Y. Onyshchenko, P. Cools, K. Ostrikov, N. De Geyter, and R. Morent. "Atmospheric-pressure plasma assisted engineering of polymer surfaces: From high hydrophobicity to superhydrophilicity." *Applied Surface Science* 535 (2021): 147032. https://doi.org/10.1016/j.apsusc.2020.147032

[5] Wahab, I. F., A. R. Bushroa, S. W. Teck, T. T. Azmi, M. Z. Ibrahim, and J. W. Lee. "Fundamentals of antifogging strategies, coating techniques and properties of inorganic materials: A comprehensive review." *Journal of Materials Research and Technology* 23 (2023): 687–714. https://doi.org/10.1016/j.jmrt.2023.01.015

[6] He, H. and Z. Guo. "Superhydrophobic materials used for anti-icing: Theory, application, and development." *iScience* 24 (2021): 103357. https://doi.org/10.1016/j.isci.2021.103357

[7] Ferrari, M., A. Benedetti, E. Santini, F. Ravera, L. Liggieri, E. Guzman, and F. Cirisano. "Biofouling control by superhydrophobic surfaces in shallow euphotic seawater." *Colloids and Surfaces A: Physicochemical and Engineering Aspects* 480 (2015): 369–375. https://doi.org/10.1016/j.colsurfa.2014.11.009

[8] Orazbayev, S. A., A. U. Utegenov, A. T. Zhunisbekov, M. Slamyiya, M. K. Dosbolayev, and T. S. Ramazanov. "Synthesis of carbon and copper nanoparticles in radio frequency plasma with additional electrostatic field." *Contributions to Plasma Physics* 58, no. 10 (2018): 961–966. https://doi.org/10.1002/ctpp.201700146

[9] Rasitha, T. P., S. Sofia, B. Anandkumar, and J. Philip. "Long-term antifouling performance of superhydrophobic surfaces in seawater environment: Effect of substrate material, hierarchical surface feature and surface chemistry." *Colloids and Surfaces A* 647 (2022): 129194. https://doi.org/10.1016/j.colsurfa.2022.129194

[10] Zheng, S., C. Li, Q. Fu, M. Li, W. Hu, Q. Wang, and Z. Chen. "Fabrication of self-cleaning superhydrophobic surface on aluminum alloys with excellent corrosion resistance." *Surface and Coatings Technology* 276 (2015): 341–348. https://doi.org/10.1016/j.surfcoat.2015.07.002

[11] Dalawai, S. P., M. A. S. Aly, S. S. Latthe, R. Xing, R. S. Sutar, S. Nagappan, C.-S. Ha, K. K. Sadasivuni, and S. Liu. "Recent advances in durability

of superhydrophobic self-cleaning technology: A critical review." *Progress in Organic Coatings* 138 (2020): 105381. https://doi.org/10.1016/j.porgcoat.2019.105381

[12] Zhao, Y., L. Lei, Q. Wang, and X. Li. "Study of superhydrophobic concrete with integral superhydrophobicity and anti-corrosion property." *Case Studies in Construction Materials* 18 (2023): e01899. https://doi.org/10.1016/j.cscm.2023.e01899

[13] Latthe, S. S., R. S. Sutar, A. K. Bhosale, K. K. Sadasivuni, and S. Liu. "Superhydrophobic surfaces for oilwater separation."*In* , 339–356. Elsevier, 2019. https://doi.org/10.1016/B978-0-12-816671-0.00016-3

[14] Lin, W., M. Cao, K. Olonisakin, R. Li, X. Zhang, and W. Yang. "Superhydrophobic materials with good oil/water separation and self-cleaning property." *Cellulose* 28 (2021): 10 425–10 439. https://doi.org/10.1007/s10570-021-04175

[15] Sun, J., J. Wang, W. Xu, and B. Zhang. "A mechanically robust superhydrophobic corrosion resistant coating with self-healing capability." *Materials & Design* 240 (2024): 112881. https://doi.org/10.1016/j.matdes.2024.112881

[16] Farhadi, S., M. Farzaneh, and S. A. Kulinich. "Anti-icing performance of superhydrophobic surfaces." *Applied Surface Science* 257 (2011): 6264–6269. https://doi.org/10.1016/j.apsusc.2011.02.057

[17] Ussenkhan, S. S., B. A. Kyrykbay, Y. Yerlanuly, A. T. Zhunisbekov, M. T. Gabdullin, T. S. Ramazanov, S. A. Orazbayev, and A. U. Utegenov. "Fabricating durable and stable superhydrophobic coatings by the atmospheric pressure plasma polymerisation of hexamethyldisiloxane." *Heliyon* 10, no. 1 (2024): e23844. https://doi.org/10.1016/j.heliyon.2023.e23844

[18] Dosbolayev, M. K., A. U. Utegenov, T. S. Ramazanov, and T. T. Daniyarov. "Structural and transport properties of dust formation in plasma of noble gases mixture in radio frequency discharge." *Contributions to Plasma Physics* 53 (2013): 426–461. https://doi.org/10.1002/ctpp.201200122

[19] Mohamed, A. M. A., A. M. Abdullah, and N. A. Younan. "Corrosion behavior of superhydrophobic surfaces: A review." *Arabian Journal of Chemistry* 8, no. 6 (2015): 749–765. https://doi.org/10.1016/j.arabjc.2014.03.006

[20] Hashjin, R. R., Z. Ranjbar, H. Yari, and G. Momen. "Tuning up solgel process to achieve highly durable superhydrophobic coating." *Surfaces and Interfaces* 33 (2022): 102282. https://doi.org/10.1016/j.surfin.2022.102282

[21] Huang, X., M. Sun, X. Shi, J. Shao, M. Jin, W. Liu, R. Zhang, S. Huang, and Y. Ye. "Chemical vapor deposition of transparent superhydrophobic anti-icing coatings with tailored polymer nanoarray architecture." *Chemical Engineering Journal* 454 (2023): 139981. https://doi.org/10.1016/j.cej.2022.139981

[22] Orazbayev, S., M. Gabdullin, T. Ramazanov, A. Zhunisbekov, and R. Zhumadilov. "Obtaining hydrophobic surfaces in atmospheric pressure plasma." *Materials Today: Proceedings* 20 (2020): 335–341. https://doi.org/10.1016/j.matpr.2019.10.071

[23] He, H., J. Du, Z. Weng, C. Fan, L. Xicai, Z. Kang, and D. Chen. "One-step electrodeposition to fabricate superhydrophobic surfaces on flexible conductive films: Optimization of metallic compounds." *Materials Today Communications* 65 (2023): 105492. https://doi.org/10.1016/j.mtcomm.2023.105492

[24] Dosbolayev, M., A. Utegenov, and T. Ramazanov. "Structural properties of buffer and complex plasmas in rf gas discharge-imposed electrostatic field." *IEEE Transactions on Plasma Science* 44 (2015): 469–472. https://doi.org/10.1109/TPS.2015.2497267

[25] Orazbayev, S., M. Muratov, T. Ramazanov, M. Dosbolayev, M. Silamiya, M. Jumagulov, and L. Boufendi. "The diagnostics of dusty plasma in rf discharge by two different methods." *Contributions to Plasma Physics* 53 (2013): 436–441. https://doi.org/10.1002/ctpp.201200123

[26] Orazbayev, S., M. Jumagulov, M. Dosbolayev, M. Silamiya, T. Ramazanov, and L. Boufendi. "Optical spectroscopic diagnostics of dusty plasma in rf discharge." *AIP Conference Proceedings* 1397 (2011): 379–380. https://doi.org/10.1063/1.3659852

[27] Abdirakhmanov, A. R., A. T. Baikaliyev, M. K. Dauylbayeva, B. A. Kyrykbay, S. A. Orazbayev, A. U. Utegenov, M. T. Gabdullin, and D. G. Batryshev. "The formation of chondrule-like particles in rf discharge plasma." *Physical Sciences and Technology* 10, no. 3–4 (2023): 68–72. https://doi.org/10.26577/phst.2023.v10.i2.08

[28] Orazbayev, S., Y. Yerlanuly, A. Utegenov, Z. Moldabekov, M. Gabdullin, and T. Ramazanov. "Plasma with carbon nanoparticles: advances and application." *Nanotechnology* 32 (2021): 455602. https://doi.org/10.1088/1361-6528/ac1a40

[29] Akhanova, N., Y. Yerlanuly, D. Batryshev, T. Kulsartov, Y. Chikhray, T. Ramazanov, A. Veziroglu, D. Schur, W. Kang, and M. Gabdullin. "The study of deuterium permeability of film-forming inhibitors with the addition of fullerenes." *International Journal of Hydrogen Energy* 46 (2021): 7426–7431. https://doi.org/10.1016/j.ijhydene.2020.11.241

[30] Akhanova, N., E.-S. Negim, Y. Yerlanuly, D. Batryshev, M. Eissa, D. Schur, T. Ramazanov, K. Azzam, M. Muratov, and M. Gabdullin. "Influence of fullerene content on the properties of polyurethane resins: A study of rheology and thermal characteristics." *Heliyon* 10 (2024): e33282. https://doi.org/10.1016/j.heliyon.2024.e33282

[31] Kyrykbay, B. A., A. R. Abdirakhmanov, S. S. Ussenkhan, A. U. Utegenov, Y. Yerlanuly, T. S. Ramazanov, T. B. Koshtybayev, and S. A. Orazbayev. "Obtaining hydrophobic coatings from ar + hmdso using radiofrequency discharge at atmospheric pressure." *International Journal of Mathematics and Physics* 15, no. 1 (2024): 77–82. https://doi.org/10.26577/ijmph.2024v15i1a9

[32] Liu, H., F. Wang, S. Lei, J. Ou, and W. Li. "Large-area fabrication of colorful superhydrophobic coatings with high solar reflectivity." *Construction and Building Materials* 304 (2021): 124602. https://doi.org/10.1016/j.conbuildmat.2021.124602

[33] Yang, X., Y. Liu, Y. Zhong, and H. Chen. "Anti/de-icing superhydrophobic coating with durability and self-healing by infiltrating photothermal self-stratifying organic layers into plasma-sprayed porous al2o313

[34] Trinh, X., D. Nguyen, M. Hossain, and Y. Mok. "Deposition of superhydrophobic coatings on glass substrates from hexamethyldisiloxane using a khz-powered plasma jet." *Surface and Coatings Technology* 361 (2019): 377–385. https://doi.org/10.1016/j.surfcoat.2019.01.068

[35] Zuza, D., V. Nekhoroshev, A. Batrakov, A. Markov, and I. Kurzina. "Characterization of hexamethyldisiloxane plasma polymerization in a dc glow discharge in an argon flow." *Vacuum* 207 (2023): 111690. https://doi.org/10.1016/j.vacuum.2022.111690

[36] Profili, J., S. Babaei, M. Al Rashidi, A. Dorris, S. Asadollahi, A. Sarkissian, and L. Stafford. "Plasma-deposited organosilicon hydrophobic coatings on cellulosic materials for wet packaging applications." *Coatings* 13 (2023): 924. https://doi.org/10.3390/coatings13050924

[37] Li, M., Z. Zhao, X. Fang, Z. Zhang, and M. Deng. "Transparent hydrophobic thermal insulation cswoznosio coatings: Energy saving, anti-dust and anti-fogging performance." *Materials Research Express* 8, no. 2 (2021): 025012. https://doi.org/10.1088/2053-1591/abe05f

Information about authors

B.A Kyrykbay *– KBTU, IASIT, e-mail: baglankyrykbaj44@gmail.com*
S.S. Ussenkhan *– KBTU, IASIT, e-mail: sultan@physics.kz*
A.Ye. Akhanova *– PhD, KBTU, Acting Vice-Rector for Science and Innovation, e-mail: n.akhanova@kbtu.kz*
A.U. Utegenov *– corresponding author, PhD, Al-Farabi KazNU, IASIT, e-mail: almasbek@physics.kz*
M.T. Gabdullin *– cand. of phys.-math. sciences, KBTU, Rector, e-mail: gabdullin@physics.kz*
S.A. Orazbayev *– PhD, Al-Farabi KazNU, IASIT, e-mail: sagi.orazbayev@gmail.com*